

Orbital Angular Momentum of Light for Chiroptical Sensing in Tissues



Igor Meglinski^{1*}, Anton Sdobnov², and Alexander Bykov²

¹Aston Institute of Photonic Technologies, Aston University, Birmingham B4 7ET, UK

²Optoelectronics and Measurement Techniques, University of Oulu, P.O. Box 4500, Oulu FI-90014, Finland

Submission: April 13, 2026; Published: April 22, 2026

*Corresponding author: Igor Meglinski, Aston Institute of Photonic Technologies, Aston University, Birmingham B4 7ET, UK

Abstract

Chiroptical sensing in biological tissue is fundamentally constrained by multiple scattering, which destroys the polarization correlations on which conventional circular dichroism, optical rotatory dispersion, and polarimetric glucose monitoring depend. This mini-review summarises recent experimental and theoretical work demonstrating that coupling molecular chirality to the topological phase structure of structured light beams carrying orbital angular momentum (OAM) generates a protected observable that survives scattering depths far exceeding polarization survival limits. Circular birefringence is transduced via spin-orbit interaction into an azimuthal rotation of the helical wavefront. Because this rotation is encoded in the topological winding of the phase rather than in the polarization state, it is preserved as a statistical ensemble invariant under strong multiple scattering (optical density of approximately 10). Differential detection between conjugate topological charges isolates the chiral contribution while cancelling the achiral background, yielding refractive-index sensitivity of order 10^{-6} . Notably, opposite glucose enantiomers produce mirror-symmetric phase maps under identical scattering conditions, confirming that molecular handedness information can survive tissue turbidity. These findings establish structured light carrying OAM as a qualitatively new and robust paradigm for non-invasive chiroptical spectroscopy and glucose sensing in turbid tissue-like highly scattering media, with emerging directions including miniaturized instrumentation, AI-assisted signal extraction, and pathways toward quantum-enhanced sensitivity.

Keywords: orbital angular momentum (OAM); chiral phase memory; glucose sensing; multiple scattering; Laguerre- Gaussian beams; circular birefringence; biophotonics; spin-orbit interaction; non-invasive diagnostics

Abbreviations: OAM: Orbital Angular Momentum; LG: Laguerre-Gaussian; CR: Conical Refraction; CD: Circular Dichroism; ORD: Optical Rotatory Dispersion; SLM: Spatial Light Modulator; MC: Monte Carlo; ML: Machine Learning;

Introduction

Optical methods for probing molecular chirality have a long history, from the first observations of optical rotation in sugar solutions to modern circular dichroism spectrophotometers capable of resolving sub-millimolar enantiomeric excess [1,2]. Yet in turbid biological media, this analytical power is fundamentally curtailed: scattering destroys the polarization correlations that carry chiroptical information within a few transport mean free paths [3]. For biological tissue, where the transport mean free path l^* is typically of order 0.5–1 mm, any technique relying on polarization state, circular dichroism, optical rotatory dispersion, Mueller-matrix polarimetry, or ellipsometry, loses sensitivity at depths of a few millimetres [4]. Non-invasive clinical chiroptical sensing, and in particular non-invasive blood glucose monitoring, has not yielded a clinically approved device despite three decades

of effort, precisely because this scattering barrier has not been overcome [5].

The recognition that different optical degrees of freedom degrade at different rates in multiple scattering has opened a new conceptual avenue [6]. Polarization state randomises rapidly, but the topological charge l of a Laguerre-Gaussian (LG) vortex beam, the integer winding number of its helical phase, was predicted and subsequently demonstrated to survive propagation through strongly scattering media with z/l^* of 10 and above [7,8]. This OAM phase memory arises because the azimuthal phase gradient of a vortex beam cannot be continuously degraded by individual scattering events; only discrete changes of topological charge are permissible. This topological robustness [9], is structurally distinct from classical angular and spatial memory effects [10], and

provides the physical foundation for a new class of measurement: one in which weak molecular interactions are transduced into a topologically protected phase observable rather than a fragile polarization signature.

The field now extends well beyond LG beams. Conical refraction (CR) in biaxial crystals has emerged as a versatile source of fractional and non-integer OAM states with continuously varying vector polarization landscapes [11], and OAM-carrying vector vortex beams, fibre-integrated modes, and meta-surface-generated structured fields are all being actively explored in the biophotonics context [12]. Concurrently, Mueller matrix polarimetry has matured into a quantitative tissue-imaging modality capable of discriminating healthy and pathological states with diagnostic accuracy approaching histopathology [13], while computational strategies, including physics-informed machine learning (ML) and next-generation Monte Carlo (MC) modelling, are enabling extraction of ever-richer information from multiply scattered structured light [14,15]. This confluence of structured-light physics, polarimetric imaging, and data-driven analysis was recently surveyed in a comprehensive studies on OAM and polarized light in biophotonics [13,16,17], which charts the field's trajectory over the coming decade.

The present mini-review focuses on one key theme within this broader landscape: the coupling of molecular chirality to OAM beam topology and the preservation of the resulting chiral phase observable through tissue- strength multiple scattering. We summarise the underlying physics, the experimental evidence, the emerging landscape of OAM sources and detection strategies, and the implications for non-invasive diagnostic sensing.

Discussion

OAM Phase Memory: Physical Basis and Broader Context

A Laguerre-Gaussian beam $LG(l,p)$ carries orbital angular momentum of hl per photon, where l is the topological charge, the integer winding number of the helical wavefront. The field phase at the detection plane decomposes into radial wavefront curvature, the helical phase term $(-l^*\varphi)$ carrying topological charge, the longitudinal propagation phase $(-kz)$, and the Gouy phase $G(z)$ [18]. The helical phase term is the topological contribution: its winding number cannot be gradually altered by a smooth perturbation and can only change by discrete amounts. In a scattering medium, random deflections of individual photons produce spatially random speckle patterns at the output, and the absolute phase at any fixed coordinate is scrambled. The azimuthal gradient $d(\psi)/d(\varphi) = -l$, however, is a global topological property of the ensemble-averaged field, preserved through z/l^* of approximately 10 as a statistical invariant [7,8].

This resilience is not equivalent to classical spatial or angular memory. The angular memory effect preserves shift- invariant tilt correlations and decays exponentially with sample thickness [10]. The polarization memory effect preserves partial circular

polarization through forward-scattering media but is absent in isotropically scattering systems [2,19]. OAM phase memory, by contrast, is observed in tissue-mimicking phantoms and *ex vivo* skin regardless of the degree of polarization of the output field, functioning as a topological invariant rather than a statistical correlation [7,8].

A critical insight from the biophotonics is that OAM robustness in tissue is not unconditional: it depends on wavelength, topological charge, beam size, tissue anisotropy, and partial coherence [20-22]. Highly forward- scattering, birefringent, and heterogeneous biological tissues impose distinct conditions compared to isotropic laboratory phantoms. A predictive framework linking tissue microstructure and OAM preservation, encompassing scattering anisotropy, absorption, birefringence, and numerical aperture, remains an open challenge requiring coordinated theoretical, computational, and experimental effort [3,23].

Spin-Orbit Transduction of Chirality into OAM Phase

When an LG beam propagates through a chiral medium characterised by circular birefringence $\Delta n_{CB}(C) = n_L(C) - n_R(C)$, spin-orbit interaction converts the polarization-dependent phase delay into an azimuthal rotation of the helical wavefront [24,25]. The chiral medium-induced phase accumulates along the spiral Poynting-vector trajectories intrinsic to OAM beams. The effective spiral interaction length $L_{spiral}(r)$ varies with radial coordinate and depends on topological charge through the geometry of the Poynting-vector flow [18,26], so that the total measured phase decomposes as [27]

$$\Psi_{meas}(C, l) = k \Delta n_{achiral}(C) L_{eff} + \text{sign}(l) k \Delta n_{CB}(C) L_{spiral} |l| .$$

where the first term is the achiral contribution (independent of the sign of l) and the second is the chiral contribution (reversing sign with l). The chiral term manifests as a coherent azimuthal rotation $\theta_{OAM} = k \Delta n_{CB}(C) L_{spiral}(r)$ of the helical phase structure, directly proportional to glucose concentration and topological charge magnitude [27].

In the broader language this constitutes a realisation of enantioselective OAM-mediated light-matter interaction, linking the chirality of the optical vortex handedness to the circular birefringence of the molecular ensemble [28,29].

Differential Detection and Enantiomer Selectivity

The achiral contribution to the total measured phase is identical for l and $-l$ beams: it arises from bulk refractive index changes, scattering-induced path elongation, and depolarization, none of which distinguish opposite helical phase gradients. Comparing phase shifts for conjugate topological charges therefore cancels the achiral background:

$$\Delta\Psi_{diff} = \Psi_{+l} - \Psi_{-l} = 2k \Delta n_{CB}(C) L_{spiral} |l|$$

isolating the glucose-specific chiral signal with doubled sensitivity [18]. The sign of $\Delta\Psi_{diff}$ encodes molecular handedness:

$D(+)$ -glucose ($\Delta n_{CB} > 0$, dextrorotatory) and $L(-)$ -glucose ($\Delta n_{CB} < 0$, levorotatory) produce equal-magnitude but oppositely directed azimuthal rotations, yielding mirror-symmetric phase maps [27]. This enantiomer selectivity is the key distinction from all achiral refractive-index sensing: only the differential handedness of the molecular structure and the helical wavefront can produce opposite signs of $\Delta\Psi_{\text{diff}}$.

The topological charge also functions as a tunable metrological parameter. Lower-order modes ($l = 3$) exhibit loosely wound Poynting-vector helices; small refractive-index perturbations produce proportionally large distortions of this gentle phase structure, yielding enhanced fractional sensitivity optimal for transparent or weakly scattering media. Higher-order modes ($l = 5$) produce tightly wound trajectories with greater absolute path length, accumulating larger absolute phase shifts and improving

signal-to-noise in strongly scattering tissue [27]. The two regimes are complementary and may be exploited within a single instrument by switching topological charge.

Experimental Validation

Experimental validation employed a modified Mach-Zehnder interferometer in which LG beams generated by a spatial light modulator traversed scattering samples before entering a cuvette containing glucose solution; interference with a reference plane wave enabled off-axis Fourier-domain phase retrieval [27]. Measurements were performed for $D(+)$ - and $L(-)$ -glucose at concentrations spanning the physiological range (50-150 mg/dl), across four scattering conditions: transparent medium ($z/l^* = 0$), low-scattering phantom ($z/l^* = 2$), strongly scattering phantom ($z/l^* = 9.6$), and *ex vivo* porcine skin (z/l^* of ~ 10 and above).

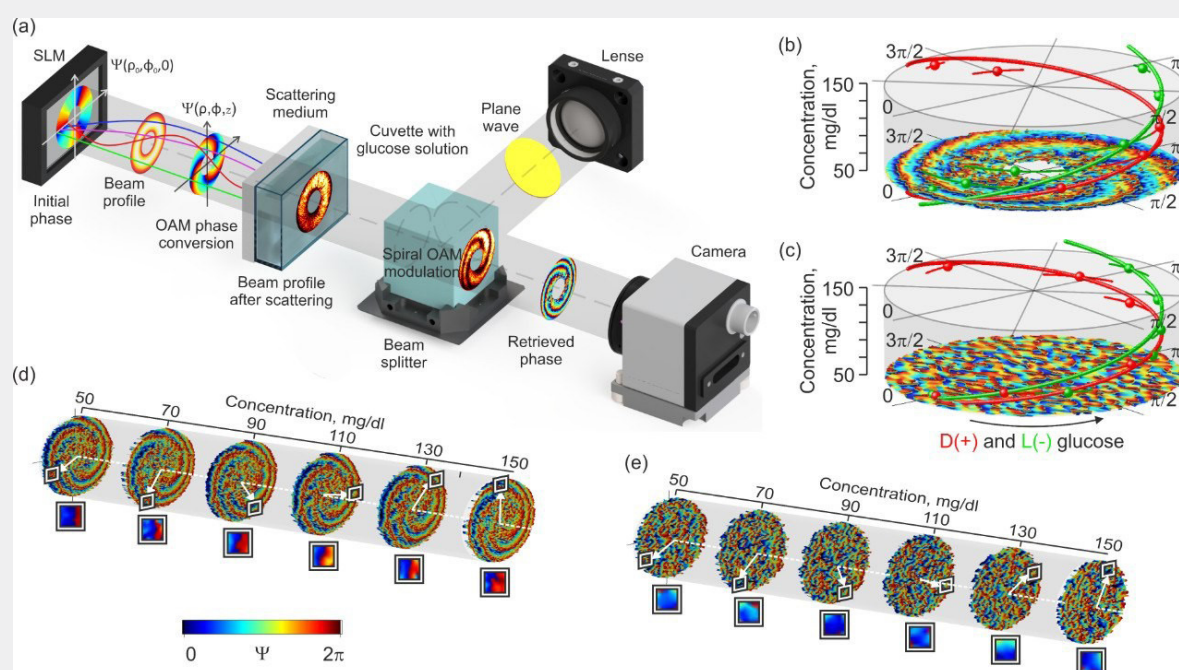


Figure 1: Schematic representation of the Mach-Zehnder interferometer experiment: the LG beam (a), carrying OAM imparted by a spatial light modulator (SLM), passes through scattering medium and cuvette containing glucose solution; interference between the transmitted LG beam and a reference plane wave is then analysed for retrieved phase distributions; OAM-related azimuthal phase shift versus glucose concentration C for nearly transparent phantom – weakly ($z/l^* = 0.1$) scattering medium (b) and *ex vivo* porcine skin – strongly ($z/l^* \approx 10$) scattering (c), measured with a Laguerre–Gaussian beam ($l = 3$). Linear fits demonstrate that the rate of azimuthal OAM twist, the topologically protected observable, preserves its quantitative relationship to glucose concentration despite a two-order-of-magnitude change in scattering strength. Error bars: standard deviation, $n = 10$ measurements. Relative OAM phase twist depending on glucose concentration in case of low scattering medium (d) and skin tissue *in vitro* (e). Adapted from [27].

Most strikingly, coupling molecular chirality to OAM beam topology generates a protected chiral phase observable that survives strong multiple scattering: the slope relating azimuthal phase rotation to glucose concentration is quantitatively preserved through *ex vivo* porcine skin ($z/l^* \approx 10$), where conventional polarimetric signals are fully destroyed, with near-identical magnitude to that measured through a nearly

transparent phantom ($z/l^* = 0.1$), an invariance spanning two orders of magnitude in scattering strength (Fig.1) [27].

The central experimental finding is that the slope relating azimuthal phase rotation to glucose concentration is preserved with near-identical magnitude across all four scattering conditions, an invariance spanning two orders of magnitude in scattering

strength [27]. The linear, calibratable response is preserved in both magnitude and sign through *ex vivo* porcine skin, where the output field consists almost entirely of speckle and the absolute phase at any fixed coordinate is fully randomised. The preserved observable is not the absolute phase but its azimuthal gradient, which survives as an ensemble statistical invariant despite local phase randomisation. In the differential ($l = \pm 5$) measurements, phase shifts between conjugate charges maintain a linear relationship with concentration through all scattering conditions, with refractive-index sensitivity of approximately 10^{-6} [27].

Enantiomer selectivity was directly demonstrated by comparing *D*(+)- and *L*(-)-glucose at identical concentrations and scattering conditions. The two enantiomers produce azimuthal rotations of opposite sign and equal magnitude, yielding mirror-symmetric polar phase plots [27]. This constitutes unambiguous experimental evidence that the measured phase shift originates from molecular chirality rather than any achiral refractive-index effect, and that OAM phase memory preserves not only the magnitude but also the sign of the circular birefringence through strongly scattering tissue.

Emerging OAM Sources: Beyond Laguerre-Gaussian Beams

The experimental demonstrations described above rely on SLM-generated LG beams, which are well-suited for laboratory implementation but face challenges of bulk size, limited power handling (damage threshold below 0.1 J/cm^2), and cost in clinical deployment. The OAM-based biophotonics identifies several alternative sources of topologically structured light that may address these constraints [11,30,31].

CR in biaxial crystals offers a particularly attractive route [11]. When a beam propagates along the optic axis of a biaxial crystal such as $\text{KGd}(\text{WO}_4)_2$, it refracts into a hollow cylinder carrying continuously tuneable fractional and non-integer OAM states with azimuthally varying polarization structure. CR systems are inherently compact (mm^3 scale), cover a broad spectral range from ultraviolet to mid-infrared, and sustain damage thresholds exceeding 10 J/cm^2 , far beyond SLM limits. Crucially, CR beams have already demonstrated refractive-index sensitivity of order 10^{-6} , comparable to LG-based results [11], and their fractional OAM states provide a spectroscopic-like topological contrast whereby each fractional charge probes a slightly different structural sensitivity regime. The dual-cone geometry may also imprint anisotropic speckle correlations linked to tissue birefringence and OAM topology, opening new diagnostic dimensions inaccessible to LG beams.

Fibre-integrated OAM sources and meta-surface-based beam shapers represent further miniaturisation pathways [30]. Optical fibres supporting OAM modes enable delivery of structured light

at the tip of an endoscope or intraoperative probe, while flat-optic meta-surfaces, including recently demonstrated meta-surface polarimeters for structural tissue imaging [30], offer alignment-tolerant, broadband, and chip-compatible OAM generation. Liquid-crystal polarization diffractive elements and *q*-plates also provide dynamic OAM generation with sub-millisecond switching, compatible with video-rate phase retrieval. Together, these developments address the compact instrumentation challenge identified as central to clinical translation [32].

Computational Modelling and AI-Accelerated Signal Extraction

A robust quantitative foundation for OAM-based chiroptical sensing requires predictive models of how topological phase observables evolve in realistic tissue geometries. Standard intensity-centric MC methods, which track scalar or vector fluence, discard precisely the phase-dependent and modal degrees of freedom that define OAM sensing. A fundamental transformation of MC frameworks [33,34] is required, evolving them into state-aware simulation engines that explicitly propagate OAM, coherence statistics, and eigenchannel structure through tissue-realistic geometries.

Key advances include the embedding of Stokes-Mueller formalism with phase-sensitive statistics, such as mutual coherence functions and modal correlation measures, into MC kernels, enabling prediction of speckle evolution, OAM memory effects, and hidden phase correlations that survive multiple scattering [15,17,35]. Eigenchannel-aware modelling, in which preferred transmission pathways through tissue are treated as intrinsic model primitives rather than emergent post-processing results, reduces model variance and stabilises inverse problems. Such frameworks are beginning to establish quantitative links between tissue microstructure parameters (scattering anisotropy, birefringence, chirality) and measurable OAM phase observables, providing the physically interpretable forward models needed to translate phase measurements into molecular concentrations.

Machine learning provides a decisive acceleration when co-designed with physics-based MC rather than used as a black-box substitute [33,34]. Physics-informed neural networks trained on MC-generated datasets enforce reciprocity, energy conservation, and Mueller-matrix constraints, improving robustness against noise and system imperfections while enabling real-time inference. In the context of OAM chiroptical sensing, ML-based phase unwrapping and azimuthal rotation estimation can suppress speckle-induced artefacts that would otherwise degrade concentration accuracy, potentially extending the usable scattering depth well beyond $z/l^* = 10$. OAM-mediated machine learning has already demonstrated high-accuracy mode-feature encoding [31], and extensions to chiral phase retrieval in turbid media are a natural next step.

Relation to the Broader Landscape: Mueller Polarimetry and Backscattering Polarimetry

OAM-based chiral phase sensing does not stand alone but complements a maturing ecosystem of polarimetric diagnostic modalities. Mueller matrix polarimetry has demonstrated clinically relevant sensitivity to tissue microstructure, collagen architecture, fibre orientation, birefringence, with diagnostic accuracy for cancer discrimination approaching histopathology in several anatomical sites including cervix, oral cavity, skin, and brain white matter [13]. Penetrative backscattering polarimetry, which polarimetrically analyses deep scattered light using a point-like laser illumination geometry, extends Mueller imaging to depth-resolved volumetric characterization of subsurface structures and has demonstrated promise for non-invasive metabolic monitoring including glucose sensing [36,37]. These modalities target complementary information: Mueller polarimetry probes structural anisotropy and depolarization; OAM phase sensing probes chirality; backscattering polarimetry probes subsurface volumetric organization.

OAM-based chiroptical sensing occupies a distinct position: it operates through strongly scattering tissue using a physical mechanism, topological phase protection, that has no counterpart in any existing optical glucose sensing modality. Where polarimetric approaches lose enantiomer selectivity within a few transport mean free paths, OAM phase memory retains it at z/l^* of 10 and above. Where Raman spectroscopy achieves molecular specificity at the cost of integration times and complex calibration models [38,39], OAM differential detection isolates chirality through a geometric cancellation requiring no molecular spectral library. Where photoacoustic depth-gated infrared methods improve depth selectivity in blood-rich dermis [40], OAM provides chiroptical specificity in a transmission geometry. These modalities are complementary, and their eventual integration within multimodal platforms represents a realistic pathway toward non-invasive tissue biochemistry at clinically relevant depths.

Toward Quantum-Enhanced OAM Chiroptical Sensing

A forward-looking direction identified in [9] is the deployment of non-classical OAM states for sensitivity enhancement beyond the classical shot-noise limit. Single-photon and two-photon entangled skyrmionic states, OAM-entangled photon pairs, and quantum-trajectory MC frameworks for modelling quantum light in complex media are all beginning to be explored. In the context of glucose sensing, the refractive-index sensitivity achieved classically (approximately 10^{-6}) already approaches the shot-noise limit for classical interferometry; quantum-enhanced schemes with NOON states or OAM-entangled pairs could, in principle,

surpass this limit through Heisenberg-scaling sensitivity [41-43]. While substantial experimental and theoretical challenges remain, including the generation, delivery, and detection of quantum-structured light in realistic tissue geometries, the conceptual framework is now sufficiently developed to motivate systematic investigation. Hybrid classical-quantum MC approaches [43] that model loss, depolarization, and mode mixing consistently across regimes provide the computational tools needed to predict where quantum enhancement becomes practically accessible.

Conclusion

Chiral phase memory, the preservation of the sign-dependent coupling between OAM beam topology and molecular circular birefringence through strong multiple scattering, represents a qualitatively new class of optical memory effect and a physically distinct approach to chiroptical sensing in turbid biological media. The key experimental results established are: (i) the azimuthal rotation of the LG beam helical wavefront is quantitatively preserved through *ex vivo* porcine skin at z/l^* of 10 and above, where conventional polarimetric signals are fully destroyed;

(ii) differential detection between conjugate topological charges cancels the achiral background and doubles chiral sensitivity, achieving refractive-index resolution of approximately 10^{-6} ; (iii) opposite glucose enantiomers produce mirror-symmetric phase maps under identical scattering conditions, confirming that handedness information survives multiple scattering encoded in a topological rather than polarimetric observable; (iv) topological charge functions as a tunable metrological parameter enabling optimisation for transparent versus strongly scattering media.

Situated within broader studies of OAM light in complex media [12,16,17], these results mark one milestone on a longer bio-sensing trajectory. The path to clinical translation will require: compact OAM generation via CR, meta-surfaces, or fibre-integrated sources capable of surviving clinical environments; state-aware MC modelling frameworks that quantitatively link tissue microstructure to OAM phase observables; physics-informed machine learning for real-time phase extraction under in vivo noise and motion; and multimodal integration with Mueller polarimetry and other complementary diagnostic modalities. Longer-term, quantum-enhanced OAM sensing may extend sensitivity beyond classical limits. The differential OAM measurement strategy generalises beyond glucose to any interaction coupling differentially to opposite topological charge signs, including magneto-optical effects, pharmaceutical enantiomer detection, and chiral signatures of biomolecular assemblies in tissue. Chiral phase memory therefore opens a broad new route for weak symmetry-breaking spectroscopy in multiply scattering environments.

Acknowledgements

This work was supported by the EU Horizon Europe EIC Pathfinder Open Research and Innovation Programme, OPTIPATH project, Grant Agreement No. 101185769, and partially by the European Cooperation in Science and Technology: Horizon 2020 COST Action CA23125: “The mETamaterial foRmalism approach to recognize cAnCer” (TETRA) and COST Action CA21159: “Understanding interaction light – biological surfaces: possibility for new electronic materials and devices” (PhoBioS), as well as by the British Council and the Department for Science, Innovation and Technology (DSIT), UK under grant project iPOL-Bio – “Integrating Polarized Light in AI-driven Biophotonics: Enhancing Health Applications”.

Conflict of Interest

The authors declare no conflict of interest.

References

- Cai H, Gu L, Hu H, Zhan Q (2025) Enhancement methods for chiral optical signals by tailoring optical fields and nanostructures. *Engineering* 45(2): 25-43.
- Monti M, Biancorosso L, Coccia E (2024) Time-resolved circular dichroism in molecules: experimental and theoretical advances. *Molecules* 29(17): 4049.
- Tuchin VV (2016) Polarized light interaction with tissues. *J Biomed Opt* 21(7): 071114.
- MacKintosh FC, Zhu JX, Pine DJ, Weitz DA (1989) Polarization memory of multiply scattered light. *Phys Rev B* 40(13): 9342-9345.
- Leung HMC, Forlenza GP, Prioleau TO, Zhou X (2023) Noninvasive glucose sensing in vivo. *Sensors* 23(16): 7057.
- Cao H, Mosk AP, Rotter S (2022) Shaping the propagation of light in complex media. *Nat Phys* 18: 994-1007.
- Meglinski I, Lopushenko I, Sdobnov A, Bykov A (2024) Phase preservation of orbital angular momentum of light in multiple scattering environment. *Light Sci Appl* 13: 214.
- Khanom F, Mohamed N, Lopushenko I, Sdobnov A, Doronin A, et al. (2024) Twists through turbidity: propagation of light carrying orbital angular momentum through a complex scattering medium. *Sci Rep* 14: 20662.
- Novikova T (2025) Preserving orbital angular momentum in scattering media. *Nat Rev Phys* 7: 470-472.
- Freund I, Rosenbluh M, Feng S (1988) Memory effects in propagation of optical waves through disordered media. *Phys Rev Lett* 61(20): 2328-2331.
- Galiakhmetova D, Mohamed N, Khanom F, Singh S, Piavchenko G, et al. (2025) Topological phase structures of conical refraction beams: expanding orbital angular momentum applications for nanoscale biosensing. *Nanophotonics* 14(24): 4447-4457.
- Forbes A, de Oliveira M, Dennis MR (2021) Structured light. *Nat Photon* 15: 253-262.
- He C, He H, Chang J, Chen B, Ma H, et al. (2021) Polarisation optics for biomedical and clinical applications: a review. *Light Sci Appl* 10: 194.
- Chae S, Huang T, Rodríguez-Núñez O, Lucas T, Vanel JC, et al. (2025) Machine learning approach to 3×4 Mueller polarimetry for complete reconstruction of diagnostic polarimetric images of biological tissues. *IEEE Trans Med Imaging* 44(9): 3820-3831.
- Ding H, Gao X, Zhang R, Guo Z (2025) Monte Carlo Simulation Method for Applications of Polarization Information Processing. *Adv Theory Simul* 8(10): e00513.
- Cheng M, Jiang W, Guo L, Li J, Forbes A (2025) Metrology with a twist: probing and sensing with vortex light. *Light Sci Appl* 14: 4
- Gigan S, Katz O, de Aguiar HB, Andresen ER, Aubry A, et al. (2022) Roadmap on wavefront shaping and deep imaging in complex media. *J Phys Photonics* 4(4): 042501
- Berry MV, McDonald KT (2008) Exact and geometrical optics energy trajectories in twisted beams. *J Opt A: Pure Appl Opt* 10(3): 035005.
- Macdonald CM, Jacques SL, Meglinski IV (2015) Circular polarization memory in polydisperse scattering media. *Phys. Rev. E* 91: 033204.
- Gianani I, Suprano A, Giordani T, Spagnolo N, Sciarrino F, et al. (2020) Transmission of vector vortex beams in dispersive media. *Adv. Photonics* 2(3): 036003.
- Krupinski-Ptaszek P, Li GY, Liu YL, et al., (2024) Robust detection technology of orbital angular momentum of partially coherent vortex light fields in complex environments. *Opto-Electron Sci* 3: 240001
- Fu Q, Zhou L, Huang X, Bai Y & Fu X (2024) Propagation dynamics of orbital angular momentum beams under the hazy scattering environment. *Opt. Express* 32(16): 27255-27267
- Jacques SL (2013) Optical properties of biological tissues: a review. *Phys. Med. Biol* 58(11): R37-R61
- Bliokh K, Rodriguez-Fortuno F, Nori F, Zayatz A (2015) Spin-orbit interactions of light. *Nat Photon* 9: 796- 808.
- Forbes KA, Andrews DL (2018) Optical orbital angular momentum: twisted light and chirality. *Opt Lett* 43(3): 435-438.
- Bliokh KY, Bekshaev AY, Kofman AG, Nori F (2013) Photon trajectories, anomalous velocities and weak measurements: a classical interpretation. *New J Phys* 15: 073022.
- Meglinski I, Sdobnov A, Bykov A (2026) Chiral phase memory of twisted light through multiple scattering. *arXiv:2602.08677*.
- Forbes KA, Green D (2024) Topological-charge-dependent dichroism and birefringence of optical vortices. *Laser Photonics Rev* 18(12): 2400109.
- Forbes KA, Andrews DL (2021) Orbital angular momentum of twisted light: chirality and optical activity. *J Phys Photonics* 3(2): 022007.
- Thrane P, Meng C, Bykov A, Sieryi O, Ding F, et al. (2026) Reflective metagrating polarimeter for single-shot full-Stokes mapping: toward digital histopathology. *Light Adv Manuf* 7: 30.
- Fang X, Hu X, Li B, Su H, Cheng K, et al. (2024) Orbital angular momentum-mediated machine learning for high-accuracy mode-feature encoding. *Light Sci Appl* 13: 49.
- Baldini F, Dholakia K, French P, Guntinas-Lichius O, Kohler A, et al. (2025) Shining a light on the future of biophotonics. *J Biophotonics* 18(7): e202500148.
- Nguyen V, Clennell A, Yakovlev VV, Doronin A (2025) NeuralRTE: Forward photon transport simulations in turbid media aided by machine learning and artificial intelligence. *Comput. Biol. Med* 185: 110892.
- Chandel S, Unni SN (2025) Deep learning-assisted identification and localization of ductal carcinoma from bulk tissue in-silico models generated through polarized Monte Carlo simulations. *Biomed. Phys. Eng. Express* 11(2): 025039.

35. Meglinski I, Tuchin VV (2025) Hidden Coherent Structure and Phase Correlations of Unpolarized Light in Multiple Scattering. *Doklady Physics* 524: 23-32.
36. Hornung M, Jain A, Frenz M, Akarçay HG (2019) Interpretation of backscattering polarimetric images recorded from multiply scattering systems: a study on colloidal suspensions. *Opt. Express* 27(5): 6210-6239.
37. Zhang X, Fan J, Song J, Zeng N, He H, et al. (2025) Depth-resolved imaging in turbid media via Mueller matrix polarimetry. *J Biomed Opt* 30(5): 056009.
38. Pors A, Rasmussen KG, Inglev R, Jendrike N, Philipps A, et al. (2023) Accurate post-calibration predictions for non-invasive glucose measurements in people using confocal Raman spectroscopy. *ACS Sensors* 8(3): 1272-1279.
39. Pors A, B Korzeniowska, Rasmussen MT, Lorenzen CV, Rasmussen KG, et al. (2025) Calibration and performance of a Raman-based device for non-invasive glucose monitoring in type 2 diabetes. *Sci Rep* 15: 10226.
40. Uluc N, Glasl S, FGasparin, T Yuan, He H et al. (2024) Non-invasive measurements of blood glucose levels by time-gating mid-infrared optoacoustic signals. *Nat Metabolism* 6: 678-686.
41. Ornelas P, Nape I, de Mello Koch R, Forbes A (2024) Non-local skyrmions as topologically resilient quantum entangled states of light. *Nat. Photonics* 18: 258-266.
42. Ma J, Yang J, Liu S, Chen B, Li X, et al. (2025) Nanophotonic quantum skyrmions enabled by semiconductor cavity quantum electrodynamics. *Nat Phys* 21: 1462-1468.
43. Besaga VR, Lopushenko IV, Sieryi O, Bykov A, Setzpfandt F, et al. (2026) Bridging classical and quantum approaches for quantitative sensing of turbid media with polarization-entangled photons. *Laser Photonics Rev* e01172.



This work is licensed under Creative Commons Attribution 4.0 License
DOI: [10.19080/CTBEB.2026.24.5560137](https://doi.org/10.19080/CTBEB.2026.24.5560137)

**Your next submission with Juniper Publishers
will reach you the below assets**

- Quality Editorial service
- Swift Peer Review
- Reprints availability
- E-prints Service
- Manuscript Podcast for convenient understanding
- Global attainment for your research
- Manuscript accessibility in different formats
(Pdf, E-pub, Full Text, Audio)
- Unceasing customer service

Track the below URL for one-step submission
<https://juniperpublishers.com/online-submission.php>